

# Effective Connectivity Network of Aberrant Prediction Error Processing in Auditory Phantom Perception

Feifan Chen<sup>1</sup>, Mansoureh Fahimi Hnazaee<sup>2</sup>, \*Sven Vanneste<sup>1,3</sup>, & Anusha Yasoda-Mohan<sup>3</sup>

<sup>1</sup> Lab for Clinical and Integrative Neuroscience, Trinity College Institute for Neuroscience, School of Psychology, Trinity College Dublin, Ireland

<sup>2</sup> Wellcome Centre for Human Neuroimaging, UCL Queen Square Institute of Neurology, London, United Kingdom

<sup>3</sup> Global Brain Health Institute, Trinity College Dublin, Ireland

## \*Correspondence to:

Sven Vanneste

Lab for Clinical and Integrative Neuroscience

Institute for Neuroscience, School of Psychology

Trinity College Dublin

College Green

Dublin 2, Ireland

*Email:* [sven.vanneste@tcd.ie](mailto:sven.vanneste@tcd.ie)

*Website:* [www.lab-clint.org](http://www.lab-clint.org)

**Keywords:** directed connectivity, predictive coding, omission response, tinnitus

## Abstract

Prediction error (PE) is key to perception in the predictive coding framework. However, previous studies indicated the varied neural activities evoked by PE in tinnitus patients. Here, we aimed to reconcile the conflict by 1) a more nuanced view of PE, which could be driven by changing of stimulus (stimulus-driven prediction error, sPE) and violation of current context (context-driven prediction error, cPE) and 2) investigating the aberrant connectivity networks that are engaged in the processing of the two types of PEs in tinnitus patients. Ten tinnitus patients with normal hearing and healthy controls were recruited and a local-global auditory oddball paradigm was applied to measure the electroencephalographic difference between the two groups during sPE and cPE conditions. Overall, the sPE condition engaged bottom-up and top-down connections, whereas the cPE condition engaged mostly top-down connections. The tinnitus group showed decreased sensitivity to the sPE and increased sensitivity to the cPE condition. Particularly, the auditory cortex and posterior cingulate cortex were the hubs for processing cPE in the control and tinnitus groups respectively showing the orientation to an internal state in tinnitus. Furthermore, tinnitus patients showed stronger connectivity to the parahippocampus and pregenual anterior cingulate cortex for the establishment of the prediction during the cPE condition. These results begin to dissect the role of changes in stimulus characteristics vs changes in the context of processing the same stimulus in mechanisms of tinnitus generation.

## Significance statement

This study delves into the number dynamics of prediction error (PE) in tinnitus, proposing a dual framework distinguishing between stimulus-driven PE (sPE) and context-driven PE (cPE). Electroencephalographic data from tinnitus patients and controls revealed distinct connectivity patterns during sPE and cPE conditions. Tinnitus patients exhibited reduced sensitivity to sPE and increased sensitivity to cPE. The auditory cortex and posterior cingulate cortex emerged as pivotal regions for cPE processing in controls and tinnitus patients, indicative of an internal state orientation in tinnitus. Enhanced connectivity to the parahippocampus and pregenual anterior cingulate cortex underscores the role of context in tinnitus pathophysiology.

## 1. Introduction

Prediction error (PE) is the mismatch between sensory input and its internal prediction generated from our previous experience (Knill and Pouget, 2004). As per the predictive coding framework, the brain is constantly minimizing PEs to optimize the internal model for better prediction of its environment (Friston, 2008). Prediction from a higher hierarchical level is encoded and sent to a lower level, whereas the PEs that emerge from the lower level will be delivered back to the higher levels for updating the prediction in order to minimise PEs. For instance, PEs are obtained when a standard, predictable stimulus (e.g. tone played 75% of the time) is interspersed with a deviant, unpredictable stimulus (e.g. noise played 25% of the time) (Garrido et al., 2009). Such a PE could be termed a *stimulus-driven PE (sPE)*, since the deviant stimulus differs from the standard, not just in probability but also in stimulus characteristics. However, it is also possible to obtain a *context-driven PE (cPE)* by comparing the neural response to the same stimulus (e.g., tone) when played in two different scenarios (75% vs 25% probability). Furthermore, context-driven PEs reflect a more 'global' effect of PE changes, which links more to the violation of expected regularity (Sergent et al., 2005). Recent accounts have articulated PEs as variates across the stimuli and contexts that also interact with each other (Bekinschtein et al., 2009; Feldman and Friston, 2010; Wacongne et al., 2011). Yet, the difference in cortical processes involving the two types of PEs remains debatable. In this work, we sought to compare the dynamic neural network underlying the modulation of stimulus and context-driven PEs and how they can explain the mechanism of phantom perceptions.

The neural responses of auditory PEs have been well established by subtracting the evoked activity of a deviant stimulus from that of a standard (Bekinschtein et al., 2009; Wacongne et al., 2011). The evoked activity pre-stimulus indicates the auditory prediction of incoming inputs (Partyka et al., 2019). The post-stimulus activities include a mismatch negativity response (MMN), an automatic response due to a change in stimulus characteristics (Garrido et al., 2009; Näätänen et al., 2007), and a late positive potential (P300) that reflects a more complex, attention-driven component of the change in stimulus (Bekinschtein et al., 2009; Polich, 2007). Although the evoked neural responses of sPEs and cPEs have been mostly explored from the studies of event-related potential (ERP), there are only a few studies investigating the neural pathway of how these PEs are communicated

between different brain regions in time (Garrido et al., 2007; Phillips et al., 2016), thus requiring further investigation.

In previous research, we showed changes in an auditory PE network during the PE processing for the tinnitus group, consisting of the parahippocampus (PHC), auditory cortex (AC), pregenual anterior cingulate cortex (pgACC), dorsal anterior cingulate cortex (dACC) and posterior cingulate cortex (PCC) (Mohan et al., 2022). The PHC plays an important role in auditory memory encoding and retrieval and in predicting incoming stimuli (Aminoff et al., 2013; Pearson et al., 2011). The dACC is an important region identified in the error-monitoring literature, particularly for novelty detection (Clark et al., 2000), which occupies a higher level in the prediction error hierarchy. The pgACC, has been identified as part of the auditory top-down “noise-cancellation” system (Rauschecker et al., 2010; Rauschecker et al., 2015) and the PCC which is the core hub of the default mode network (DMN), is indicated to be activated when PE is detected (Leech and Sharp, 2014; Mohan et al., 2022; Pearson et al., 2011). From a neural oscillation perspective, PE is fed forward in the theta frequency band (4–7.5 Hz) (Recasens et al., 2018), which plays a role in the processing of novel stimuli (Hsiao et al., 2009; Ko et al., 2012). Whereas predictions of upcoming stimuli are fed back through alpha (8–12 Hz) connectivity (Recasens et al., 2018). Oscillations in the alpha band also link with the active inhibition modulation that is also influenced by the top-down regulation based on context and previous experience (Alamia and VanRullen, 2019; Jensen et al., 2012).

Spatiotemporal neural responses of sPEs and cPEs and how they are communicated between the regions of the PE network can be used to study the mechanism of action of chronic phantom percepts such as tinnitus. For a long time, tinnitus has been explained under the predictive coding framework (De Ridder et al., 2014; Hullfish et al., 2019; Sedley et al., 2016). Under this theory, tinnitus is regarded as a maladaptive compensation of PEs, where PEs are either generated through changes in the incoming sensory information as a result of maladaptive changes in the auditory system (Sedley et al., 2016) or owing to relatively strong top-down priors generated by the auditory memory and noise-cancelling mechanisms (De Ridder et al., 2014). For those with hearing loss but no tinnitus, their noise gating system is hypothesised to successfully minimise the PE by suppressing the increased neural noise, whereas for those with tinnitus but normal hearing, the deficient noise

cancellation system fails to inhibit (or falsely relay) the irrelevant neural noise to the sensory cortex (Leaver et al., 2011; Rauschecker et al., 2010), where the PE is minimised by active adaptation. Only recently there is growing empirical evidence for this theory. Recent findings of changes in MMN and P300 responses in tinnitus patients indicated their sensitivity to PEs (Mohan et al., 2021; Sedley et al., 2019). However, it is still not clear if the generation of tinnitus or any phantom perception maybe bottom up – i.e. sensitive to changes in input, as suggested by a lot of the previous literature (Noreña and Farley, 2013; Schaette and McAlpine, 2011), to be driven by changes to the sensory pathways or if it's more top-down – i.e. sensitive to changes in the context in which the same stimulus is processed. Therefore, by examining sPEs and cPEs we may attempt to answer these questions.

Here, we aimed to investigate the network connectivity that is associated with aberrant processing of PEs in tinnitus patients with slight audiometric hearing loss. We hypothesised that 1) distinct time-varying connectivity networks would be observed in processing sPE and cPE and 2) compared to the control group, tinnitus patients would manifest aberrant connectivity networks in processing sPE and cPE, especially centred around PHC, pgACC and PCC as suggested by the previous studies (Mohan et al., 2022; Vanneste et al., 2019). Based on the theory above that patients with little changes in the auditory pathways exhibit changes in top-down processing, we expect tinnitus patients in the current study to be more sensitive to top-down PEs a.k.a. cPEs (De Ridder et al., 2014; Vanneste et al., 2019). This is not only a systematic approach to exploring the dynamic prediction error network and its perceptual consequence in tinnitus, but also a foundational step to understanding the mechanism of action of the phantom percepts in other modalities (De Ridder et al., 2014; Mohan and Vanneste, 2017).

## 2. Methods

### 2.1 Participants

Ten tinnitus participants whose tinnitus lasted more than 1 year were recruited in this study. Ten healthy controls were recruited from the local community. The sample is based on our previously published study (Mohan et al., 2022). The two groups were matched for age, gender and hearing loss. All participants' hearing thresholds were measured using pure

tone audiometry. Those who showed a hearing threshold larger than 30 dB HL at any frequency were excluded from the study. The other exclusion criteria included Meniere's disease, chronic ear infections, otosclerosis, tumours, mental disorders, chronic headache, and pulsatile tinnitus. All participants gave written consent to participate.

## *2.2 Audiological and behavioural assessments*

All participants underwent a pure tone audiometry test where hearing thresholds at 250, 500, 1000, 2000, 3000, 4000, 6000, and 8000 Hz were obtained according to the procedures prescribed by the British Society of Audiology.

Furthermore, two 10-cm visual analogue scales (VAS) were applied to measure the tinnitus loudness and tinnitus-related distress. The two VAS scales were scored from 0 to 10 with 0 of "no tinnitus"/"no distress" and 10 of "as loud as imaginable"/"suicidal levels of distress". Tinnitus participants also completed a set of questionnaires, including the Tinnitus Handicap Inventory (Newman et al., 1996) (THI;  $M \pm SD = 29 \pm 24.8$ ), Tinnitus Questionnaire (Hallam et al., 1988), and Tinnitus Functional Index (Meikle et al., 2012), which are also designed to assess tinnitus-related distress and impact on their lives.

Additional audiometric evaluations were conducted within the tinnitus group to ascertain the pitch and loudness of each participant's tinnitus perception. Two pure tones at varying frequencies were played at 10 dB above the participant's hearing threshold at those frequencies, and the participant was asked to choose the tone that best matched the pitch of their tinnitus. This selected tone was then played alongside another tone of a different frequency, and the participant repeated the matching process. This procedure was repeated until the frequency that most accurately matched the pitch of the participant's tinnitus was determined ( $M = 3361.11$  Hz,  $SD = 2837.01$  Hz). The loudness of the tinnitus was established by adjusting the presentation level of the matched tone until the participant indicated that it matched the loudness of their tinnitus. The loudness level was recorded as the difference between the matched level and the audiometric threshold at that frequency in the tested ear. The stimuli for both procedures were presented to the ear opposite the tinnitus ear (or the ear with the more severe tinnitus, in cases of bilateral tinnitus).

### 2.3 Auditory Oddball Paradigm

The design of the oddball paradigm was adapted from an original study by Wacongne and colleagues (Wacongne et al., 2011). We applied three sound sequences such that the Sequence X included five 500 Hz tones, the Sequence Y included four tones and a noise burst and the Sequence Omission included four tones with the fifth stimulus absent (**Figure 1**). The tones and noise bursts were 50ms long with a rise-fall time of 7ms and an interstimulus interval of 250ms. The stimuli were presented at 72 dB SPL. All audio files were produced by Cool Edit Pro. As shown in Figure 1, each trial started with a 1250 ms sound sequence followed by a random inter-trial jitter between 700 – 1000ms.

The paradigm consisted of two protocols and each protocol had seven blocks of 125 trials. In the xxxxx protocol (n = 7 blocks), Sequence X was the standard and Sequence Y worked as the deviant. In the xxxxY protocol (n = 7 blocks), Sequence Y was standard and Sequence X worked as the deviant and Sequence Omission was the omission sequence in both. Each block started with 25 standard sequences and the following 100 trials included 75% standard trials, 15% deviant trials and 10% omission trials (**Figure 1**). The omission protocol (n = 1 blocks) which included 125 omission trials was presented towards the end to avoid habituation to the omission. The participants could take breaks between subsequent blocks and between subsequent protocols. Based on our previous study (Mohan et al., 2022) and the original study (Wacongne et al., 2011), we know that the xxxxY protocol directly measures the global effect of the brain encoding the entire sequence vs just the independent stimuli. Therefore, our analyses in this paper will be based on the xxxxY and omission protocol considering three basic conditions i.e. standard (**Figure 1g**), unexpected omission (**Figure 1i**) and expected omission (**Figure 1j**).

### 2.4 EEG pre-processing

The stimuli were presented through the Neuroscan Stim II system which triggered the Neuroscan Scan 4.5 Acquire software. EEG was recorded using 64-channel Neuroscan Synamps2 Quick Cap configured per the International 10–20 placement system with a reference close to Cz (impedance < 5k $\Omega$ ). The data was then sampled using the Neuroscan Synamps2 amplifier at 500 Hz and online band-pass filtered at 0.1–70 Hz. Participants were

asked to refrain from caffeine before the study. During the test, they were required to keep their eyes fixed on the fixation cross on the screen and minimize body movement.

EEG data was then pre-processed using EEGLAB (Delorme and Makeig, 2004) and ERPLAB (Lopez-Calderon and Luck, 2014) toolboxes in MATLAB. The pipelines for EEG pre-processing included removing unused and bad channels by visual inspection, re-referencing to average reference, and filtering between 0.5 and 44 Hz. Data was epoched between -100 ms to 1850 ms relative to the onset of the first tone in each sequence. The epoched data was then subjected to temporal independent component analysis (ICA) to remove muscle artefacts, eye blinks, saccades, and other noise transients (tinnitus: range = 8-24, median: 18; control: range = 15-29, median = 18.5). No group difference in the number of artefact ICA was observed ( $t(18) = 1.396, p = .179$ ). Artefacts in all epochs were detected and deleted using a simple voltage threshold of  $\pm 90\mu\text{V}$  and manual inspection. The channels initially removed were interpolated using a spherical interpolation algorithm in EEGLAB (tinnitus: range = 1-7, median: 3; control: range = 1-5, median = 1) before the ICA. No group difference in the number of interpolated channels was observed ( $t(18) = 1.462, p = .161$ ).

### 2.5 Source localization and ROIs

All trials for all the conditions were source localized for the entire time length using the Brainstorm toolbox (Tadel et al., 2011). The ICBM-1522 template was used to create the head model and the forward model was generated using OpenMEEG BEM. The noise covariance matrix was calculated based on the baseline of all trials. Source reconstruction was performed using dynamic statistical parametric mapping (dSPM) with a fixed source orientation constraint where the vertex normal to the source space solution is applied (Hämäläinen, 2010). We selected 10 regions of interest (ROIs) based on previous studies (Mohan et al., 2022), which were left and right AC (BA 41), left and right parahippocampus (BA 36), left and right pgACC/vmPFC (BA 24), left and right dACC (BA 32) and left and right PCC (BA 31). The size of ROIs was standardized to 10 cm<sup>2</sup>. The network was then visualized by BrainNet Viewer toolbox (Xia et al., 2013).

## 2.6 Granger Causality

Granger Causality (GC) is used to capture the amount of information and the direction of information transfer between different regions. GC aims to measure the statistical probability of past activity causing future activity (Granger, 1969), which has become a popular method for connectivity that resists noise and predefined connections (Friston et al., 2014). The time-varying effective connectivity between the ROIs was calculated using partial directed coherence (PDC) (Baccalá and Sameshima, 2001), which is a Granger causality measure in the frequency-domain. A set of process in the observed time series are defined as a multivariate autoregressive (MVAR) model:

$$y(n) = \sum_{k=1}^p A_k(n)y(n-k) + w(n) \quad (1)$$

, where  $y \in R^{m \times N \times T}$  represents the ERP data format as ROIs ( $m$ ) by time points ( $N$ ) by trials ( $T$ ),  $n$  represents the  $n$ -th time point in single trials and  $p$  is the model order that determines the maximum number of lagged time points in the MVAR model.  $w(n)$  is Gaussian distributed white noise with zero mean.  $A_k$  comprises the coefficients  $a_{ijk}$  that reflect the linear relationship the ROI  $i$  and ROI  $j$  at the time lag  $k$  ( $i, j = 1, \dots, 10, k = 1, \dots, p$ ).  $A_k$  was estimated by using a multi-trial adaptation of the General Linear Kalman Filter (GLKF) (Milde et al., 2010), which outperforms other available algorithms in inferring the time-varying causal influence with high sampling rate (Pagnotta and Plomp, 2018). A model order of 25 (time lag of 50 ms) and adaptation coefficient of 0.01 were chosen as the parameters of time-varying GC after parameter exploration using multiple criteria in the previous study (Fahimi Hnazaee et al., 2020). From equation 1, PDC can be measured as (Baccala et al., 2007):

$$\pi_{i \rightarrow j}(f, n) = \frac{\bar{A}_{ij}(f, n)}{\sqrt{\sum_{r=1}^m \bar{A}_{jr}(f, n) \bar{A}_{jr}^*(f, n)}} \quad (2)$$

where  $f$  ranges from 0 to the maximum frequency limit ( $f_{max}$ ) so the spectral density matrix  $\bar{A}_{ij}(f, n)$  is the Fourier transform of the  $A_k$  coefficients:

$$\bar{A}_{ij}(f, n) = I - \sum_{k=1}^p A_k(n) e^{-2j\pi f k}$$

where  $I$  is the identity matrix that  $I = 1$  when  $i = j$  and  $I = 0$  otherwise.  $\bar{A}^*$  represents the complex conjugate. Thus,  $\pi_{i \rightarrow j}(f, n)$  ranges from 0 to 1 with higher value implying higher Granger causal from ROI  $i$  to ROI  $j$  at  $n$ -th time bin and  $f$ -th frequency bin.

## 2.7 Statistical analysis

### 2.7.1 Removal of spurious connections

PDC of the standard, expected omission and unexpected omission conditions in tinnitus and control groups were calculated first by the multi-trial adaptation. The  $f_{max}$  was set as 44 Hz in line with the low-pass filter settings. The number of frequency bins was set as 500. This step resulted in a four-dimensional matrix of PDC values for each subject (10 x 10 brain connectivity x 500 frequency bins x 975 time points).

To test for statistically significant non-zero connections for each subject, a null distribution by randomizing the phase information while preserving the amplitude distribution was performed. This phase randomization was done using a fast-Fourier transform (FFT) and inverse FFT was performed to obtain the surrogate data. This was implemented using the SIFT toolbox in EEGLAB (Delorme et al., 2011). The estimated connectivity from the actual data was then compared to the connectivity estimated from the surrogate data (null distribution) using the cluster-based permutation test with 100 of randomisation ( $\alpha = 0.05$ , two-tailed), in which clusters were defined as data points per time bins and frequency to control for the family-wise error rate (FWER). Consequently, the spurious GC was ruled out for each subject by only including estimated connectivity that is significantly larger than the surrogate data in further analysis. This method has been validated in previous studies (Fahimi Hnazaee et al., 2020; Kamiński et al., 2001).

Previous research has suggested that the communication of the prediction is encoded in the alpha band connectivity and that of the PE in the theta band connectivity (Recasens et al., 2018). Therefore the PDC matrices in the theta (4 – 7.5 Hz) and alpha frequency (8–12 Hz) bands were extracted and averaged around respective frequency bins for each subject, generating a 10 x 10 x 975 PDC matrix for each subject in each group (controls, tinnitus),

condition (standard, unexpected omission, expected omission) and frequency band (theta, alpha).

### 2.7.2 Within-group analysis

To determine the significance of condition-level difference in each group and frequency band, a dependent-sample permutation test with 1000 randomisations was conducted. In each randomisation, the data (10 x 10 x 975) of two compared conditions were first pooled (unexpected omission vs standard or unexpected vs expected omission). Then, the pooled data was fully shuffled and randomly assigned to create PDC matrices for the two compared conditions. This permutation process was repeated each group (controls, tinnitus) and each frequency band (theta, alpha). This resulted in 8 statistical tests: 2 condition pairs x 2 frequency bands x 2 groups. Thus, alpha level for the difference was selected as  $\alpha = 0.00625$  (0.05/8) for each test after correcting for multiple comparisons using a Bonferroni correction.

### 2.7.3 Between-group analysis

To investigate the group difference of the time-varying connectivity network during the hierarchical PE processing, the sPE and cPE were analysed. The four dimensional PDC matrix of sPE (i.e. unexpected omission – standard) and cPE (i.e. unexpected omission – expected omission) for each subject was calculated. Then, the PDC matrix for the sPE and cPE in the theta (4 – 7.5 Hz) and alpha frequency (8–12 Hz) bands were averaged across the respective frequency bins in each subject. To determine the group difference in the connectivity during the sPE and cPE processing, in each PE condition and frequency band, an independent-sample permutation test with 1000 randomisations was conducted. In each randomisation, the data (10 x 10 x 975) of two groups were first pooled (tinnitus vs control). Then, the pooled data was fully shuffled and randomly assigned to create PDC matrices for the two groups. This permutation process was repeated each conditions (sPE, cPE) and each frequency band (theta, alpha). To ensure a strict correction we used the same alpha level as for the within-subject analysis  $\alpha = 0.00625$  (0.05/8) for each test after correcting for multiple comparisons using a Bonferroni correction. The effect size (Cohen's *d*) was estimated as an indication of the strength of group difference. The results showed consistently large effect

across all significant connection in all conditions and all frequency bands (Cohen's  $d$  range: sPE theta = 1.33 – 2.56, sPE alpha = 1.33 – 2.72, cPE theta = 1.36 – 2.94, cPE alpha = 1.36 – 2.80).

### 2.8 Visualisation

Per the design (**Figure 1**), the first four stimuli are similar in the standard, deviant and omission sequences, of which the fourth stimulus of all trials end at 950 ms after the first stimulus. Subsequently, the difference in stimulation conditions results in different levels of PE. Therefore, we only visualised the time-varying connectivity preceding and succeeding the fifth stimulus. Four time frames were defined based on the previous evidence and rationale: 1) the 250ms before the onset of the fifth stimulus, which we define as a pre-deviant response (PDR), 2) 0-100 ms after the onset of the fifth stimulus, hereby referred to as early deviant response (DR) (Luck, 2014; Wacongne et al., 2011), 3) 100 to 250ms after the onset of fifth stimulus that corresponds to MMN timeframe (Mohan et al., 2022; Wacongne et al., 2011) and 4) 250 to 600ms after the onset of fifth stimulus corresponding to the P300 timeframe in both the PE conditions (Mohan et al., 2022; Wacongne et al., 2011).

The time-varying connectivity per 50 ms from 250ms pre-fifth stimulus to 600ms post-fifth stimulus was first visualised at the within-group and between-group levels (see **supplementary results and Figure 1-6**). The connectivity that lasted two or more times within a specific timeframe were presented using solid lines, whereas those occurred only one time within a specific timeframe were presented using translucent lines. The number of indegrees indicated the number of connectivity directed into individual ROIs within individual time windows. For easier visualisation, the results were further condensed for four time windows: PDR, DR, MMN and P300 for each group and group difference, as shown in the result section. The connectivity that lasted two or more times within a specific timeframe were presented. The number of indegrees indicated the number of connectivity directed into individual ROIs within individual time windows.

### 3. Results

#### 3.1 Demographical results

Ten tinnitus participants (25.90±5.49 years, 8 males:2 females) and ten control participants (27.00±4.71, 4 males: 6 females) were recruited. The demographic characteristics were compared between the two groups (**Table 1**). There was no significant difference in age (**Figure 2a**) ( $t(18) = 0.48$ ,  $d = 0.21$ ,  $95\%CI = [-0.66,1.09]$ ,  $p=.63$ ) and sex (**Figure 2b**) ( $\chi^2=3.33$ ,  $p=.06$ ) between the two groups. Furthermore, two groups were matched for the hearing thresholds at every frequency in individual ears (**Figure 2c**) ( $F(7,112) = .94$ ,  $p=.48$ ,  $partial\eta^2 = .05$ ,  $95\%CI = [0,.08]$ ) and there was no significant difference in the mean hearing loss between the control ( $M\pm SD = 7.28\pm 4.72$  dB HL) and tinnitus ( $M\pm SD = 7.62 \pm 4.72$  dB HL) groups (**Figure 2d**) ( $F(3,17) = .02$ ,  $p = .89$ ,  $95\%CI = [-.83,.96]$ , one missing value).

The tinnitus characteristics were measured using audiological measures and two 10-cm VAS (**Table 1**). The audiological measures demonstrated high-frequency tinnitus pitch ( $M\pm SD = 3.36 \pm 2.84$  kHz) and the mean loudness match as  $24.33 \pm 14.85$  dB SL. The VAS showed that the mean tinnitus loudness was  $2.25 \pm 1.22$ , and tinnitus-related distress was  $1.13 \pm 1.20$ . Tinnitus participants also completed a set of questionnaires, including the THI ( $M \pm SD = 29 \pm 24.8$ ), TQ ( $M \pm SD = 24.67 \pm 12.88$ , one missing value), and TFI ( $M \pm SD = 27.48 \pm 19.47$ ).

The results of ERP, topographical maps and source localization for sPE and cPE and the group difference were published and presented in a previous study (Mohan et al., 2022).

#### 3.2 Connectivity analysis

##### 3.2.1 Time-varying connectivity

The time-varying connectivity with the time window of 50 ms was visualised at both within-group analysis and between-group analysis level. The details of results were reported in the **supplementary results** section.

##### 3.2.2 Stimulus-driven PE condition

The PDC matrix of standard and unexpected omission were compared within the tinnitus and control group first. Then, the PDC matrix of sPE were compared between the two

groups. All repetitive connectivity that showed significant difference two or more times within a specific timeframe, was summarised in **Figure 3**.

In the tinnitus group (**Figure 3a**), during PDR we observed a general decrease in alpha connectivity from and to the left PHC in the unexpected omission condition ( $n = 8$ ). Apart from that, the PCC also received decreased connectivity from the right dACC in the unexpected omission condition. By contrast, increased information was sent from the right PHC and left AC to the left dACC. During DR, there was decreased theta connectivity from the right AC to the left PHC, left dACC and right PCC for the unexpected omission condition, while increased information from the left PHC to the left dACC. During the MMN timeframe, there was increased theta information from the right pgACC, right PCC and right dACC to the AC ( $n = 8$ ) in the unexpected omission condition, while decreased one from the right dACC to the right PCC. During the P300 timeframe, we observed increased theta connectivity from the dACC to the right PCC ( $n = 4$ ) in the unexpected omission condition, whereas decreased information from the AC to the left PCC ( $n = 8$ ). The bilateral PCC sent decreased theta information to the right PHC, and the right dACC sent decreased information to the left PHC in the unexpected omission condition. In addition, there was increased theta connectivity from the right pgACC to the right AC.

The connectivity network of the control group was shown in **Figure 3b**. The results showed increased bottom-up connectivity network from the bilateral AC to other regions in all timeframes in the unexpected omission condition relative to the standard condition. During PDR, there was an increased alpha connectivity network from the AC to the PCC ( $n = 24$ ) and from the pgACC to the right dACC, AC and PCC in the unexpected omission condition. We also observed increased alpha connectivity from the right PHC to the right dACC but decreased connectivity from the left dACC to the left PHC ( $n = 11$ ). During DR, there was a general increased theta connectivity mainly from the left AC and right PHC for the unexpected omission condition. The left dACC received decreased theta information from the right pgACC and right dACC. During MMN, we observed increased theta connectivity from the left pgACC, left PHC and bilateral AC to the right PCC ( $n = 20$ ) in the unexpected omission condition but decreased connectivity within dACC and from the left dACC to the left PHC. During P300, we observed increased theta connectivity network mainly from the left AC and bilateral PHC to the dACC ( $n = 31$ ) and right PCC ( $n = 20$ ) and decreased

connectivity from the right dACC to bilateral pgACC in the unexpected omission condition. There is also a general increase in theta connectivity to the right AC (n = 19) and right PHC (n = 10).

The group difference during the processing of sPE was further investigated and presented (**Figure 3c**). In general, the tinnitus group showed decreased information transfer between the prediction error network than control group in all time frames. During PDR, compared to controls, the tinnitus group showed a general decrease in the alpha connectivity to the right AC (n = 6), right PHC (n = 10) and bilateral PCC (n = 24) from other regions. By contrast, the tinnitus group only showed increased connectivity from the left PHC to the left dACC. During DR, the left AC and left PHC of tinnitus sent decreased theta information to the right PHC relative to controls (n = 5). Tinnitus group also showed decreased theta connectivity network from the AC or left PHC to the right pgACC and right PHC than controls but increased connectivity within the dACC (n = 4). During MMN, we observed a general decrease in the theta connectivity mainly from left AC, left PHC and bilateral pgACC to the right AC (n = 9) and bilateral PCC (n = 16) in the tinnitus group compared to controls. During P300, there was still a general decrease in theta connectivity from and to the right AC (n = 10) and bilateral PCC (n = 24) for the tinnitus group. We also observed decreased theta connectivity to the right PHC (n = 9), left dACC (n = 8) and pgACC (n = 24) in tinnitus group. Interestingly, all connectivity from the right dACC to the pgACC increased for tinnitus group relative to the control group.

### 3.2.2 Context-driven PE condition

All repetitive connectivity for each group and the group difference in the cPE condition were summarized in **Figure 4**. In the tinnitus group (**Figure 4a**), most connectivity was consistently toward the right PHC, right pgACC and the right PCC which were the central hubs in processing cPEs in the tinnitus group. During PDR, there was a general increase in the alpha connectivity to the right PCC (n = 81) but decreased connectivity from the left PCC for the unexpected omission condition. We observed a decrease in the alpha connectivity to the right PHC (n = 17) and right pgACC (n = 16) but increased connectivity from these regions to the rest of the network. During DR, we observed all increased theta connectivity was sent to the right PCC (n = 23) for the unexpected omission condition relative to the

expected omission condition. In addition, the right PHC received decreased theta connectivity from the left PCC and right AC (n = 11) and sent less to the right pgACC. During MMN and P300, there was still a general increase in the theta connectivity to the right PCC but decreased connectivity to the right PHC and pgACC.

The connectivity network of the control group in the cPE condition was shown in **Figure 4b**. We observed that the right AC is the central hub in processing cPEs in the control group across all timeframes. During PDR, there was a general increase in the alpha connectivity to the right AC (n = 22), right PCC (n = 4) and right dACC (n = 6) for the unexpected omission condition but decreased connectivity to the left PCC (n = 10). In addition, the left dACC received less information from the right AC and right PCC. During DR, we observed all theta connectivity to the right AC (n = 9) increased from the bilateral PHC and right dACC for the unexpected omission condition relative to the expected omission condition. During MMN, there was still a general increase in theta connectivity mainly to the right AC (n = 25). The right PCC received increased theta information from the bilateral dACC but sent less information to the left PCC. In addition, the left dACC received less information from the right PHC and right dACC. During P300, there was still a general increase in theta connectivity to the right AC (n = 79) for the unexpected omission condition.

The group difference in the cPE condition was summarized in **Figure 4c**. In particular, the group difference of connectivity network during the processing of cPE mainly lies in right AC, right PHC and bilateral PCC. During PDR, the tinnitus group showed a general increase in alpha connectivity to the bilateral PCC (n = 59) but decreased connectivity from the left PCC to the right AC (n = 13) and left pgACC (n = 6). In addition, we also observed a general decrease in the alpha connectivity to the right AC (n = 13) and right PHC (n = 15) for the tinnitus group. During DR, compared to controls, the tinnitus group showed a general increase in theta connectivity to the left PCC (n = 13). The right AC received decreased theta information from the left PCC and sent decreased on to the left pgACC. During MMN, the bilateral PCC (n = 34) received increased theta connectivity from the bilateral AC and left pgACC, and decreased connectivity from the right PHC. We also observed a general decrease in theta connectivity to the right AC (n = 7). During P300, there was still a general increase in theta connectivity to the bilateral PCC (n = 65) but decreased connectivity from them to the right AC (n = 42) and bilateral PHC (n = 20). The right AC and right PHC also received a

decrease in theta information from the rest of the network. In addition, there was increased connectivity to the right dACC from the left pgACC. There was also decreased connectivity to the pgACC from the left dACC and the left PHC.

#### 4. Discussion

Predictive coding is recognized by several researchers to be involved in adaptive and maladaptive perceptual processes (Barron et al., 2020; De Ridder et al., 2014; Gilbert et al., 2022; Knill and Pouget, 2004). Particularly, phantom perception in different sensory domains has been regarded as a maladaptive compensation to minimize PE (Mohan and Vanneste, 2017). For example, tinnitus is explained under the predictive coding framework where it is hypothesised that the brain maladaptively compensates for the prediction error possibly induced by changes in the auditory pathways or cortical structure and function with a sound as a means to minimise the resulting uncertainty (De Ridder et al., 2014; De Ridder and Vanneste, 2021; Hullfish et al., 2019; Sedley et al., 2016). Some researchers suggested that auditory phantom perception is driven by the brain's oversensitivity to changes in the input (Sedley et al., 2016), while others propose it is driven by the brain's strong prediction of the environment (Corlett et al., 2019).

The current study tested both these hypotheses using *stimulus-driven* and *context-driven* prediction errors (sPE, cPE) in a group of chronic tinnitus patients with minimal to no auditory damage as measured by an audiogram, in comparison to a group with no tinnitus. Our findings suggest that the tinnitus group was less sensitive (decreased connectivity strength) to changes in the stimulus (sPE condition) and more sensitive (increased connectivity strength) to changes in the context in which the same stimulus was presented (cPE condition). A graphical abstract was plotted to summarise the main findings (**Figure 5**).

##### 4.1 Effect of changing stimulus characteristics on the PE network in controls and tinnitus

In the current study, the sPE was generated by subtracting the ERP to the standard (xxxxY) from the ERP of the omission (xxxx\_) where the 5<sup>th</sup> stimulus was different from the standard in both stimulus characteristics and probability. From the connectivity pattern in the control group, we observe that the PE generated by the absence of the 5<sup>th</sup> stimulus instigates the signaling of the PCC by the auditory regions (AC, PHC) in all time frames. This suggests that

the signaling of the internal default mode network in response to an unexpected absence of a stimulus is a normal process. However, the stark difference observed between the controls and tinnitus group is the increased connectivity from the top-down regions (pgACC) to the AC and/or PCC, during the pre- and post-deviant responses which is significantly reduced in the tinnitus group. This dysfunctional functioning of the top-down system in tinnitus has been consistently reported by several studies (Araneda et al., 2018; Leaver et al., 2011; Seydell-Greenwald et al., 2012) and also as a possible reason for tinnitus generation in people with minimal auditory damage (Vanneste et al., 2019). Modulating pgACC activity using tDCS (Vanneste and De Ridder, 2011) or TRT (Kim et al., 2016) has been shown to improve tinnitus symptoms.

The second major difference we observe between the connectivity patterns of the control and tinnitus groups is that the establishment of the expectation of the standard stimulus during the PDR time frame, is passed from the dACC to PHC in the control group, but from the PHC to dACC in the tinnitus group. This aligns with previous evidence showing that the dACC not only simply monitors the errors but also participates in a process to statistically predict events (Ide et al., 2013; Sallet et al., 2007). Furthermore, the PHC plays a more receptive role in controls by receiving information about the PE, whereas it plays a more active role in sending information to establish the prediction in the tinnitus group. This supports the idea that the PHC plays a key role in establishing tinnitus, as suggested by De Ridder and colleagues (De Ridder et al., 2011), some of our previous work with resting state studies (Mohan et al., 2018; Vanneste and De Ridder, 2016), and others with intracranial recordings (Sedley et al., 2015).

The signalling of the dACC by the rest of the predictive coding network in the control group becomes most apparent during the P300 time frame in line with previous literature showing its role in orienting stimulus-driven attention (Han and Marois, 2014). During this time, we also observed an increase in information transfer to the right AC, right PHC and right PCC showing right lateralisation of the P300 response. This is in consensus with previous literature showing a right lateralisation in auditory oddball tasks that is consistent with theories of right hemisphere network to be prominently involved in sustained attention, stimulus evaluation, target detection and working memory/context updating (Gilmore et al., 2009). In the tinnitus group, we observe that this right lateralisation is non-

existent, and when compared to the control group that shows decreased connectivity within the same regions.

From a task perspective, it is important to consider that the tinnitus group hears a phantom sound, and the control group does not. Therefore, when the omission stimulus was played, the tinnitus group had an ongoing internal sound while the controls did not. From this, we could speculate that the tinnitus itself may be filling in the omitted information, thereby reducing the magnitude of the prediction error and therefore its sensitivity to it. This is evident not only from the decreased sensitivity in the right hemisphere network compared to controls but also in the number of overall connections in the tinnitus group for recoding the sPE. Our findings are also in line with other literature showing reduced sensitivity to detect PEs in patients with phantom perception (McCleery et al., 2018; Sedley et al., 2019). In addition, previous studies consistently reported decreased MMN (Mahmoudian et al., 2013; Sedley et al., 2019) and P300 (Asadpour et al., 2018) amplitudes to sPE in tinnitus patients relative to controls.

On the other hand, we observe increased connectivity between the left and right dACC and from the bilateral dACC to the bilateral pgACC in the tinnitus group during the P300. This suggests increased salience as a result of the absence of the 5<sup>th</sup> stimulus as shown by previous studies (De Ridder et al., 2011; Vanneste et al., 2010a; Vanneste and De Ridder, 2012). However, this increased salience is accompanied by decreased connectivity from the pgACC to the AC and PCC in the tinnitus compared to the control and increased connectivity from the dACC to the PCC in the tinnitus group while processing the sPE in the same time frame. Therefore, these results imply that this increased salience due to the omission of the 5<sup>th</sup> stimulus may be compensated by attention directed to the internal state – i.e. perceiving the tinnitus sound – which is also in line with previous findings (Sedley et al., 2019).

#### *4.2 Effect of changes in context of the same stimulus on the PE network in controls and tinnitus*

In the current study, cPE is generated by subtracting the ERP of the expected omission of the 5<sup>th</sup> stimulus from the unexpected omission of the 5<sup>th</sup> stimulus. Therefore, the changes in controls, tinnitus and difference analyses indicate the neural markers related purely to the change in expectation of the same stimulus – i.e., when xxxx\_ is and is not the

established context. Context can be extracted from the configuration of sensory information, which facilitates the recognition of a target stimulus (Kveraga et al., 2007; Sanocki, 1993) and is important for building an expectation of the external world (Aminoff et al., 2013). As the changing of contexts requires the violation of expected regularity rather than detailed information of stimulus, cPEs are more dominated by top-down modulation. This is evident from the increased connectivity to the right AC and right PCC in the control and tinnitus groups from the rest of the PE network in all time frames respectively.

However, we observe that when `xxxx_` is the established context, there is increased connectivity to the PHC and the pgACC in the tinnitus group suggesting that these regions are key in encoding a perfectly predictable stimulus compared to the same stimulus when it is unpredictable. This is in accordance with previous literature showing that the PHC is at the core storing the sensory memory trace (Aminoff et al., 2007) and that the pgACC is responsible for updating the context (Will et al., 2017). This effect is not observed in the control group and the effect observed in the tinnitus group is significantly different from the control group. The stronger connectivity to the PHC and pgACC from the rest of the PE network during the establishment of the context of the predictable compared to the unpredictable stimulus alludes to the strong prior hypothesis of Powers and colleagues (Corlett et al., 2019) which states that hallucinations are driven by the formation of strong predictions of the environment which cannot be easily updated (Powers et al., 2017).

Another notable difference in the processing of the cPE between the control and tinnitus groups is the increased connectivity to the AC in the control group and to the PCC in the tinnitus group. The dynamic process of DMN helps convey the narrative content of information (Baldassano et al., 2018), which is linked with high-level PE that is associated with the expectation of regularity in the current context or the environment. Recent accounts have articulated the important role of the PCC in detecting sensory changes and driving subsequent shifts in self-referential processing and thus behaviour based on Bayesian inference (Pearson et al., 2011). This emphasises the importance of assessing the behavioural relationship through an intrinsic process, which is believed to be modulated by the DMN. Increased connectivity to the PCC in the current study may indicate the orientation to an internally ongoing process (Leech and Sharp, 2014). Furthermore, previous evidence also demonstrated the aberrant connectivity within and between DMN and other

networks in patients with phantom perception (Broyd et al., 2009; Chen et al., 2017; Vanneste et al., 2010b; Zhao et al., 2018). The increased activity of PCC has been observed in tinnitus compared to healthy controls and negatively correlated with the subjective loudness of tinnitus (Ueyama et al., 2013), suggesting the PCC's involvement in the maladaptive neural processes underpinning tinnitus perception. Thus, the PCC-dependent network in the tinnitus group may indicate an inordinate orientation to endogenous context (i.e., the perception of the ongoing tinnitus sound) during cPE processing.

Additionally, we observe that the increased connectivity from the dACC and pgACC is communicated to the AC in the control group and to the PCC in the tinnitus group. This suggests a different compensation mechanism for the increased salience due to cPE in the controls and tinnitus. While in the controls, the dACC searches for more information in the auditory network in the control group, it searches for more information in the DMN in the tinnitus group. The pgACC subsequently sends the changes in context to these regions as well. This, along with evidence from previous literature (Sedley et al., 2019), shows that perceiving tinnitus becomes the new default state of the brain.

#### *4.3 Changes in sPE and cPE in relevance to the mechanism of action of phantom perception in other sensory domains*

The expectation of a stimulus met with its unexpected absence, which is sPE, is reflective of a changing sensory environment. Here we observe that patients with a phantom percept (even in the presence of minimal sensory damage) are less sensitive to such a changing environment, indicating that their chronic phantom percept is now possibly filling in for the missing sensory information in the same domain. From a neural correlate perspective, we observe an increase in salience, driven by the dACC, decreased compensation by the pgACC, and a loss of right lateralisation in response to the processing of oddballs. Future studies are required to see if similar patterns of connectivity are able to predict the occurrence of an illusory percept when participants with no chronic phantom perception are subjected to an increasingly unpredictable sensory environment. In addition, more direct evidence by using fMRI, brain stimulation or animal models is expected to cross validate the current findings.

However, patients with phantom perceptions are more sensitive to the same stimulus presented in different contexts, which are cPEs. In fact, when stimulus-related changes are

removed, it becomes clear that those patients show a stronger tendency to establish the prediction of a perfectly predictable stimulus than controls suggesting that phantom perception may be generated as a result of a strong, undeterrable prediction of its environment. Furthermore, changing the context of such a strong prediction in chronic phantom perception results in the orientation to an internal state (network central at PCC), rather than to a sensory domain (network central at AC) as observed in controls. Future studies, testing the strong prior hypothesis as explained by Powers and colleagues (Corlett et al., 2019; Powers et al., 2017) may provide more concrete evidence for this mechanism of tinnitus generation.

In an earlier paper from our lab, we hypothesised that phantom percepts from different sensory domains may be a compensation of a PE produced in the appropriate sensory domains, or a domain-general PE network (Mohan and Vanneste, 2017). Investigating the sPEs and cPEs, gives us an idea of different responses that are dependent and independent respectively of changes in stimulus characteristics. For example, similar patterns of changes for sPEs and cPEs in the somatosensory domain for chronic pain patients in comparison to a control group would confirm that phantom perception in different sensory domains is a result of an aberration of a more general predictive coding system, with domain-specific compensation to the PE. This is a very powerful tool, since we will then be able to start investigating domain-general treatments for aberrant predictive coding, which can be adapted to different sensory systems, or may be able to transcend the sensory domain altogether.

#### *4.3 Limitations and future implications*

Notably, there are several limitations that need to be considered. One significant limitation of the current study is the small sample size, with ten tinnitus patients and ten healthy controls. Although the results cannot be generalised to the entirety of tinnitus population, it serves as a good pilot for future studies to invest in the investigation of network connectivity as an indicator of mechanism of action in phantom perception.

It is also important to note that while there was no significant difference in sex between the two groups, the contrast in sex distribution needs to be considered given the potential sex effect on the PE processing and related connectivity network (Fujimoto et al., 2016).

Thus, future studies should aim to include larger sample sizes and balanced sex distribution to validate and extend the current findings.

The dSPM and minimum-norm imaging estimates by Brainstorm produce an L2-minimum norm estimate of current density produced using a fixed source orientation constraint. However, Ghumare et al. (2018) suggests different ways of source localisation and there is quite a bit of discussion, from our understanding, on choosing a particular method that is best practice (Ghumare et al., 2018). Therefore, we acknowledge that the results of the current study may be constrained to the parameters chosen here. However, to confirm the results, we need future research to replicate the current results using other parameters of source localisation and Granger Causality to provide more concrete evidence to the findings.

Although hearing loss may not be a major factor driving connectivity changes in the current study, it is not possible to rule this out completely. There is substantial research suggesting the presence of cochlear synaptopathy in people with normal hearing thresholds (Bharadwaj et al., 2019; Chen et al., 2021). Furthermore, it is possible that these people have hearing loss in the frequencies higher than 8 kHz, which was not tested in this study. Therefore, future studies should note these factors during study design.

Notably, the current study only concentrated on the alpha and theta frequency bands since the communication of PEs through connectivity is proposed to be within these bands. However, predictions have been shown to be encoded also through the activity in low-beta (14-15 Hz) oscillations and PEs in gamma oscillations (> 30 Hz) (Arnal et al., 2011; Arnal and Giraud, 2012). Combining the two, it might be interesting for future studies to combine activity in high frequencies and connectivity in low frequencies to deepen the investigation on the communication of predictions and PEs through cross-frequency coupling.

Despite these limitations, the findings of this study have several potential clinical applications. Understanding the distinct patterns of predictive coding in tinnitus patients can inform the development of targeted therapies. For instance, the observed decreased sensitivity to sPEs and increased sensitivity to cPEs suggest that interventions could be tailored to modulate these specific neural processes. One potential way is the use of neuromodulation techniques, such as transcranial direct current stimulation (tDCS) (Song et al., 2012) or transcranial magnetic stimulation (TMS) (De Ridder et al., 2005), which have shown potential in modulating brain activity in tinnitus patients and tinnitus management.

By targeting regions like the pgACC or dACC, these techniques could help recalibrate maladaptive predictive coding processes and alleviate tinnitus symptoms.

## 5. Conclusion

In conclusion, sPEs and cPEs could be used as a way to test the top-down and bottom-up predictive coding process in phantom perception, like tinnitus. In the control group, while the dynamic network of sPEs reflects the integrated processing of bottom-up sensory inputs and top-down prediction, the contextual difference mainly drives a general increase of connectivity to the right AC through the top-down pathway. Interestingly, the tinnitus group showed a DMN-dominant network during cPE with increased connectivity to the PCC suggesting a powerful dependence on internal prediction. The group difference in the connectivity network may further support the maladaptive changes in prediction error processing in tinnitus patients and potential effects of tinnitus on perceptual processing. As sPE arise, a general decrease in the responsive connectivity network of tinnitus patients compared to controls may reflect the decreased sensitivity to sPE, due to the less magnitude of novelty caused by the constant perception of tinnitus. On the contrary, the strong orientation to internal prediction modulated by the increased connectivity to the PCC but decreased one from it is consistent with the increased sensitivity to cPEs of tinnitus patients. Through this study, we develop a powerful tool that can be tested in other sensory domains, to confirm if phantom perception may be domain-specific or part of a more general predictive coding system.

## Author Contributions

F.C.: Data analysis, writing manuscript, M.F.H.: Coding Granger Causality and connectivity, Data interpretation, manuscript revision, S.V.: Ideation, supervision, experimental design, A.Y.M.: Data collection, supervision, writing manuscript.

## Conflict of interest

None of the authors have potential conflicts of interest to be disclosed.

## Acknowledgement

F.C. is funded by Trinity College Dublin Postgraduate Research Studentship, M.F.H. is funded by Non-Clinical Post Doctorial Fellowship from the Guarantors of Brain (grant number: 183328) and A.Y.M. was funded by the Government of Ireland Postdoctoral Fellowship 2020-2022 (grant number: GOIPD/2020/663). These funding sources had no further roles in study design; in the collection, analysis and interpretation of data; in the writing of the report; and in the decisions to submit the paper for publication. The authors thank Colum Ó Sé for his assistance with data plotting.

## References

- Alamia A and VanRullen R. Alpha Oscillations and Traveling Waves: Signatures of Predictive Coding? *PLOS Biol* 2019;17(10):e3000487; doi: 10.1371/journal.pbio.3000487.
- Aminoff E, Gronau N and Bar M. The Parahippocampal Cortex Mediates Spatial and Nonspatial Associations. *Cereb Cortex* 2007;17(7):1493–1503; doi: 10.1093/cercor/bhl078.
- Aminoff EM, Kveraga K and Bar M. The Role of the Parahippocampal Cortex in Cognition. *Trends Cogn Sci* 2013;17(8):379–390; doi: 10.1016/j.tics.2013.06.009.
- Araneda R, Renier L, Dricot L, et al. A Key Role of the Prefrontal Cortex in the Maintenance of Chronic Tinnitus: An fMRI Study Using a Stroop Task. *NeuroImage Clin* 2018;17:325–334; doi: 10.1016/j.nicl.2017.10.029.
- Arnal LH and Giraud A-L. Cortical Oscillations and Sensory Predictions. *Trends Cogn Sci* 2012;16(7):390–398; doi: 10.1016/j.tics.2012.05.003.
- Arnal LH, Wyart V and Giraud A-L. Transitions in Neural Oscillations Reflect Prediction Errors Generated in Audiovisual Speech. *Nat Neurosci* 2011;14(6):797–801; doi: 10.1038/nn.2810.
- Asadpour A, Alavi A, Jahed M, et al. Cognitive Memory Comparison Between Tinnitus and Normal Cases Using Event-Related Potentials. *Front Integr Neurosci* 2018;12.
- Baccalá LA and Sameshima K. Partial Directed Coherence: A New Concept in Neural Structure Determination. *Biol Cybern* 2001;84(6):463–474; doi: 10.1007/PL00007990.
- Baccala LA, Sameshima K and Takahashi DY. Generalized Partial Directed Coherence. In: 2007 15th International Conference on Digital Signal Processing 2007; pp. 163–166; doi: 10.1109/ICDSP.2007.4288544.
- Baldassano C, Hasson U and Norman KA. Representation of Real-World Event Schemas during Narrative Perception. *J Neurosci* 2018;38(45):9689–9699; doi: 10.1523/JNEUROSCI.0251-18.2018.

Barron HC, Auztulewicz R and Friston K. Prediction and Memory: A Predictive Coding Account. *Prog Neurobiol* 2020;192:101821; doi: 10.1016/j.pneurobio.2020.101821.

Bekinschtein TA, Dehaene S, Rohaut B, et al. Neural Signature of the Conscious Processing of Auditory Regularities. *Proc Natl Acad Sci U S A* 2009;106(5):1672–1677; doi: 10.1073/pnas.0809667106.

Bharadwaj HM, Mai AR, Simpson JM, et al. Non-Invasive Assays of Cochlear Synaptopathy - Candidates and Considerations. *Neuroscience* 2019;407:53–66; doi: 10.1016/j.neuroscience.2019.02.031.

Broyd SJ, Demanuele C, Debener S, et al. Default-Mode Brain Dysfunction in Mental Disorders: A Systematic Review. *Neurosci Biobehav Rev* 2009;33(3):279–296; doi: 10.1016/j.neubiorev.2008.09.002.

Chen F, Zhao F, Mahafza N, et al. Detecting Noise-Induced Cochlear Synaptopathy by Auditory Brainstem Response in Tinnitus Patients With Normal Hearing Thresholds: A Meta-Analysis. *Front Neurosci* 2021;15:778197; doi: 10.3389/fnins.2021.778197.

Chen YC, Xia W, Chen H, et al. Tinnitus Distress Is Linked to Enhanced Resting-State Functional Connectivity from the Limbic System to the Auditory Cortex. *Hum Brain Mapp* 2017;38(5):2384–2397; doi: 10.1002/hbm.23525.

Clark VP, Fannon S, Lai S, et al. Responses to Rare Visual Target and Distractor Stimuli Using Event-Related fMRI. *J Neurophysiol* 2000;83(5):3133–3139; doi: 10.1152/jn.2000.83.5.3133.

Corlett PR, Horga G, Fletcher PC, et al. Hallucinations and Strong Priors. *Trends Cogn Sci* 2019;23(2):114–127; doi: 10.1016/j.tics.2018.12.001.

De Ridder D, Elgoyhen AB, Romo R, et al. Phantom Percepts: Tinnitus and Pain as Persisting Aversive Memory Networks. *Proc Natl Acad Sci U S A* 2011;108(20):8075–80; doi: 10.1073/pnas.1018466108.

De Ridder D and Vanneste S. Chapter 15 - The Bayesian Brain in Imbalance: Medial, Lateral and Descending Pathways in Tinnitus and Pain: A Perspective. In: Progress in Brain Research. (Langguth B, Kleinjung T, De Ridder D, et al. eds). Tinnitus - An Interdisciplinary Approach Towards Individualized Treatment: Towards Understanding the Complexity of Tinnitus Elsevier; 2021; pp. 309–334; doi: 10.1016/bs.pbr.2020.07.012.

De Ridder D, Vanneste S, Weisz N, et al. An Integrative Model of Auditory Phantom Perception: Tinnitus as a Unified Percept of Interacting Separable Subnetworks. *Neurosci Biobehav Rev* 2014;44:16–32; doi: 10.1016/j.neubiorev.2013.03.021.

De Ridder D, Verstraeten E, Van der Kelen K, et al. Transcranial Magnetic Stimulation for Tinnitus: Influence of Tinnitus Duration on Stimulation Parameter Choice and Maximal Tinnitus Suppression. *Otol Neurotol* 2005;26(4):616; doi: 10.1097/01.mao.0000178146.91139.3c.

Delorme A and Makeig S. EEGLAB: An Open Source Toolbox for Analysis of Single-Trial EEG Dynamics Including Independent Component Analysis. *J Neurosci Methods* 2004;134(1): 9–21.

Delorme A, Mullen T, Kothe C, et al. EEGLAB, SIFT, NFT, BCILAB, and ERICA: New Tools for Advanced EEG Processing. *Comput Intell Neurosci* 2011;2011:130714; doi: 10.1155/2011/130714.

Fahimi Hnazaee M, Khachatryan E, Chehrazad S, et al. Overlapping Connectivity Patterns during Semantic Processing of Abstract and Concrete Words Revealed with Multivariate Granger Causality Analysis. *Sci Rep* 2020;10(1):2803; doi: 10.1038/s41598-020-59473-7.

Feldman H and Friston KJ. Attention, Uncertainty, and Free-Energy. *Front Hum Neurosci* 2010;4:215; doi: 10.3389/fnhum.2010.00215.

Friston K. Hierarchical Models in the Brain. *PLOS Comput Biol* 2008;4(11):e1000211; doi: 10.1371/journal.pcbi.1000211.

Friston KJ, Bastos AM, Oswal A, et al. Granger Causality Revisited. *NeuroImage* 2014;101:796–808; doi: 10.1016/j.neuroimage.2014.06.062.

Fujimoto T, Okumura E, Kodabashi A, et al. Sex Differences in Gamma Band Functional Connectivity Between the Frontal Lobe and Cortical Areas During an Auditory Oddball Task, as Revealed by Imaginary Coherence Assessment. *Open Neuroimaging J* 2016;10:85–101; doi: 10.2174/1874440001610010085.

Garrido MI, Kilner JM, Kiebel SJ, et al. Dynamic Causal Modelling of Evoked Potentials: A Reproducibility Study. *NeuroImage* 2007;36(3):571–580; doi: 10.1016/j.neuroimage.2007.03.014.

Garrido MI, Kilner JM, Stephan KE, et al. The Mismatch Negativity: A Review of Underlying Mechanisms. *Clin Neurophysiol* 2009;120(3):453–463; doi: 10.1016/j.clinph.2008.11.029.

Ghumare EG, Schrooten M, Vandenberghe R, et al. A Time-Varying Connectivity Analysis from Distributed EEG Sources: A Simulation Study. *Brain Topogr* 2018;31(5):721–737; doi: 10.1007/s10548-018-0621-3.

Gilbert JR, Wusinich C and Zarate CA. A Predictive Coding Framework for Understanding Major Depression. *Front Hum Neurosci* 2022;16:787495; doi: 10.3389/fnhum.2022.787495.

Gilmore CS, Clementz BA and Berg P. Hemispheric Differences in Auditory Oddball Responses during Monaural versus Binaural Stimulation. *Int J Psychophysiol* 2009;73(3):326–333; doi: 10.1016/j.ijpsycho.2009.05.005.

Granger CWJ. Investigating Causal Relations by Econometric Models and Cross-Spectral Methods. *Econometrica* 1969;37(3):424–438; doi: 10.2307/1912791.

Hallam RS, Jakes SC and Hinchcliffe R. Cognitive Variables in Tinnitus Annoyance. *Br J Clin Psychol* 1988;27(3):213–222; doi: 10.1111/j.2044-8260.1988.tb00778.x.

Hämäläinen M. MNE Software User's Guide Version 2.7.3. 2010.

Han SW and Marois R. Functional Fractionation of the Stimulus-Driven Attention Network. *J Neurosci* 2014;34(20):6958–6969; doi: 10.1523/JNEUROSCI.4975-13.2014.

Hsiao F-J, Wu Z-A, Ho L-T, et al. Theta Oscillation during Auditory Change Detection: An MEG Study. *Biol Psychol* 2009;81(1):58–66; doi: 10.1016/j.biopsycho.2009.01.007.

Hullfish J, Sedley W and Vanneste S. Prediction and Perception: Insights for (and from) Tinnitus. *Neurosci Biobehav Rev* 2019;102:1–12; doi: 10.1016/j.neubiorev.2019.04.008.

Ide JS, Shenoy P, Yu AJ, et al. Bayesian Prediction and Evaluation in the Anterior Cingulate Cortex. *J Neurosci* 2013;33(5):2039–2047; doi: 10.1523/JNEUROSCI.2201-12.2013.

Jensen O, Bonnefond M and VanRullen R. An Oscillatory Mechanism for Prioritizing Salient Unattended Stimuli. *Trends Cogn Sci* 2012;16(4):200–206; doi: 10.1016/j.tics.2012.03.002.

Kamiński M, Ding M, Truccolo WA, et al. Evaluating Causal Relations in Neural Systems: Granger Causality, Directed Transfer Function and Statistical Assessment of Significance. *Biol Cybern* 2001;85(2):145–157; doi: 10.1007/s004220000235.

Kim SH, Jang JH, Lee S-Y, et al. Neural Substrates Predicting Short-Term Improvement of Tinnitus Loudness and Distress after Modified Tinnitus Retraining Therapy. *Sci Rep* 2016;6(1):29140; doi: 10.1038/srep29140.

Knill DC and Pouget A. The Bayesian Brain: The Role of Uncertainty in Neural Coding and Computation. *Trends Neurosci* 2004;27(12):712–719; doi: 10.1016/j.tins.2004.10.007.

Ko D, Kwon S, Lee G-T, et al. Theta Oscillation Related to the Auditory Discrimination Process in Mismatch Negativity: Oddball versus Control Paradigm. *J Clin Neurol Seoul Korea* 2012;8(1):35–42; doi: 10.3988/jcn.2012.8.1.35.

Kveraga K, Ghuman AS and Bar M. Top-down Predictions in the Cognitive Brain. *Brain Cogn* 2007;65(2):145–168; doi: 10.1016/j.bandc.2007.06.007.

Leaver AM, Renier L, Chevillet MA, et al. Dysregulation of Limbic and Auditory Networks in Tinnitus. *Neuron* 2011;69(1):33–43; doi: 10.1016/j.neuron.2010.12.002.

Leech R and Sharp DJ. The Role of the Posterior Cingulate Cortex in Cognition and Disease. *Brain* 2014;137(1):12–32; doi: 10.1093/brain/awt162.

Lopez-Calderon J and Luck SJ. ERPLAB: An Open-Source Toolbox for the Analysis of Event-Related Potentials. *Front Hum Neurosci* 2014;8.

Luck SJ. *An Introduction to the Event-Related Potential Technique, Second Edition*. MIT Press; 2014.

Mahmoudian S, Farhadi M, Najafi-Koopae M, et al. Central Auditory Processing during Chronic Tinnitus as Indexed by Topographical Maps of the Mismatch Negativity Obtained with the Multi-Feature Paradigm. *Brain Res* 2013;1527:161–173; doi: 10.1016/j.brainres.2013.06.019.

McCleery A, Wynn JK, Mathalon DH, et al. Hallucinations, Neuroplasticity, and Prediction Errors in Schizophrenia. *Scand J Psychol* 2018;59(1):41–48; doi: 10.1111/sjop.12413.

Meikle MB, Henry JA, Griest SE, et al. The Tinnitus Functional Index: Development of a New Clinical Measure for Chronic, Intrusive Tinnitus. *Ear Hear* 2012;33(2):153; doi: 10.1097/AUD.0b013e31822f67c0.

Milde T, Leistriz L, Astolfi L, et al. A New Kalman Filter Approach for the Estimation of High-Dimensional Time-Variant Multivariate AR Models and Its Application in Analysis of Laser-Evoked Brain Potentials. *NeuroImage* 2010;50(3):960–969; doi: 10.1016/j.neuroimage.2009.12.110.

Mohan A, De Ridder D, Idiculla R, et al. Distress-Dependent Temporal Variability of Regions Encoding Domain-Specific and Domain-General Behavioral Manifestations of Phantom Percepts. *Eur J Neurosci* 2018;48(2):1743–1764; doi: 10.1111/ejn.13988.

Mohan A, Luckey A, Weisz N, et al. Predisposition to Domain-Wide Maladaptive Changes in Predictive Coding in Auditory Phantom Perception. *NeuroImage* 2022;248:118813; doi: 10.1016/j.neuroimage.2021.118813.

Mohan A and Vanneste S. Adaptive and Maladaptive Neural Compensatory Consequences of Sensory Deprivation—From a Phantom Percept Perspective. *Prog Neurobiol* 2017;153:1–17; doi: 10.1016/j.pneurobio.2017.03.010.

Nääätänen R, Paavilainen P, Rinne T, et al. The Mismatch Negativity (MMN) in Basic Research of Central Auditory Processing: A Review. *Clin Neurophysiol Off J Int Fed Clin Neurophysiol* 2007;118(12):2544–2590; doi: 10.1016/j.clinph.2007.04.026.

Newman CW, Jacobson GP and Spitzer JB. Development of the Tinnitus Handicap Inventory. *Arch Otolaryngol Head Neck Surg* 1996;122(2):143–148; doi: 10.1001/archotol.1996.01890140029007.

Noreña AJ and Farley BJ. Tinnitus-Related Neural Activity: Theories of Generation, Propagation, and Centralization. *Hear Res* 2013;295:161–171; doi: 10.1016/j.heares.2012.09.010.

Pagnotta MF and Plomp G. Time-Varying MVAR Algorithms for Directed Connectivity Analysis: Critical Comparison in Simulations and Benchmark EEG Data. *PLOS ONE* 2018;13(6):e0198846; doi: 10.1371/journal.pone.0198846.

Partyka M, Demarchi G, Roesch S, et al. Phantom Auditory Perception (Tinnitus) Is Characterised by Stronger Anticipatory Auditory Predictions. 2019;869842; doi: 10.1101/869842.

Pearson JM, Heilbronner SR, Barack DL, et al. Posterior Cingulate Cortex: Adapting Behavior to a Changing World. *Trends Cogn Sci* 2011;15(4):143–151; doi: 10.1016/j.tics.2011.02.002.

Phillips HN, Blenkmann A, Hughes LE, et al. Convergent Evidence for Hierarchical Prediction Networks from Human Electroencephalography and Magnetoencephalography. *Cortex J Devoted Study Nerv Syst Behav* 2016;82:192–205; doi: 10.1016/j.cortex.2016.05.001.

Polich J. Updating P300: An Integrative Theory of P3a and P3b. *Clin Neurophysiol Off J Int Fed Clin Neurophysiol* 2007;118(10):2128–2148; doi: 10.1016/j.clinph.2007.04.019.

Powers AR, Mathys C and Corlett PR. Pavlovian Conditioning-Induced Hallucinations Result from Overweighting of Perceptual Priors. *Science* 2017;357(6351):596–600; doi: 10.1126/science.aan3458.

Rauschecker JP, Leaver AM and Mühlau M. Tuning out the Noise: Limbic-Auditory Interactions in Tinnitus. *Neuron* 2010;66(6):819–26; doi: 10.1016/j.neuron.2010.04.032.

Recasens M, Gross J and Uhlhaas PJ. Low-Frequency Oscillatory Correlates of Auditory Predictive Processing in Cortical-Subcortical Networks: A MEG-Study. *Sci Rep* 2018;8(1):14007; doi: 10.1038/s41598-018-32385-3.

Sallet J, Quilodran R, Rothé M, et al. Expectations, Gains, and Losses in the Anterior Cingulate Cortex. *Cogn Affect Behav Neurosci* 2007;7(4):327–336; doi: 10.3758/cabn.7.4.327.

Sanocki T. Time Course of Object Identification: Evidence for a Global-to-Local Contingency. *J Exp Psychol Hum Percept Perform* 1993;19(4):878–898; doi: 10.1037//0096-1523.19.4.878.

Schaette R and McAlpine D. Tinnitus with a Normal Audiogram: Physiological Evidence for Hidden Hearing Loss and Computational Model. *J Neurosci* 2011;31(38):13452–13457.

Sedley W, Alter K, Gander PE, et al. Exposing Pathological Sensory Predictions in Tinnitus Using Auditory Intensity Deviant Evoked Responses. *J Neurosci Off J Soc Neurosci* 2019;39(50):10096–10103; doi: 10.1523/JNEUROSCI.1308-19.2019.

Sedley W, Friston KJ, Gander PE, et al. An Integrative Tinnitus Model Based on Sensory Precision. *Trends Neurosci* 2016;39(12):799–812; doi: 10.1016/j.tins.2016.10.004.

Sedley W, Gander PE, Kumar S, et al. Intracranial Mapping of a Cortical Tinnitus System Using Residual Inhibition. *Curr Biol* 2015;25(9):1208–1214; doi: 10.1016/j.cub.2015.02.075.

Sergent C, Baillet S and Dehaene S. Timing of the Brain Events Underlying Access to Consciousness during the Attentional Blink. *Nat Neurosci* 2005;8(10):1391–1400; doi: 10.1038/nn1549.

Seydell-Greenwald A, Leaver AM, Turesky TK, et al. Functional MRI Evidence for a Role of Ventral Prefrontal Cortex in Tinnitus. *Brain Res* 2012;1485:22–39; doi: 10.1016/j.brainres.2012.08.052.

Song J-J, Vanneste S, Van de Heyning P, et al. Transcranial Direct Current Stimulation in Tinnitus Patients: A Systemic Review and Meta-Analysis. *Sci World J* 2012;2012(1):427941; doi: 10.1100/2012/427941.

Tadel F, Baillet S, Mosher JC, et al. Brainstorm: A User-Friendly Application for MEG/EEG Analysis. *Comput Intell Neurosci* 2011;2011:e879716; doi: 10.1155/2011/879716.

Ueyama T, Donishi T, Ukai S, et al. Brain Regions Responsible for Tinnitus Distress and Loudness: A Resting-State fMRI Study. *PLoS ONE* 2013;8(6):e67778; doi: 10.1371/journal.pone.0067778.

Vanneste S, Alsalman O and De Ridder D. Top-down and Bottom-up Regulated Auditory Phantom Perception. *J Neurosci* 2019;39(2):364–378; doi: 10.1523/jneurosci.0966-18.2018.

Vanneste S and De Ridder D. Bifrontal Transcranial Direct Current Stimulation Modulates Tinnitus Intensity and Tinnitus-Distress-Related Brain Activity. *Eur J Neurosci* 2011;34(4):605–614; doi: 10.1111/j.1460-9568.2011.07778.x.

Vanneste S and De Ridder D. The Auditory and Non-Auditory Brain Areas Involved in Tinnitus. An Emergent Property of Multiple Parallel Overlapping Subnetworks. *Front Syst Neurosci* 2012;6:31; doi: 10.3389/fnsys.2012.00031.

Vanneste S and De Ridder D. Deafferentation-Based Pathophysiological Differences in Phantom Sound: Tinnitus with and without Hearing Loss. *NeuroImage* 2016;129:80–94; doi: 10.1016/j.neuroimage.2015.12.002.

Vanneste S, Plazier M, der Loo E, et al. The Neural Correlates of Tinnitus-Related Distress. *NeuroImage* 2010a;52(2):470–80; doi: 10.1016/j.neuroimage.2010.04.029.

Vanneste S, Plazier M, van der Loo E, et al. The Differences in Brain Activity between Narrow Band Noise and Pure Tone Tinnitus. *PLoS One* 2010b;5(10):e13618; doi: 10.1371/journal.pone.0013618.

Wacongne C, Labyt E, van Wassenhove V, et al. Evidence for a Hierarchy of Predictions and Prediction Errors in Human Cortex. *Proc Natl Acad Sci* 2011;108(51):20754–20759; doi: 10.1073/pnas.1117807108.

Will G-J, Rutledge RB, Moutoussis M, et al. Neural and Computational Processes Underlying Dynamic Changes in Self-Esteem. *FeldmanHall O. ed. eLife* 2017;6:e28098; doi: 10.7554/eLife.28098.

Xia M, Wang J and He Y. BrainNet Viewer: A Network Visualization Tool for Human Brain Connectomics. *PLoS ONE* 2013;8(7):e68910; doi: 10.1371/journal.pone.0068910.

Zhao Z, Li X, Feng G, et al. Altered Effective Connectivity in the Default Network of the Brains of First-Episode, Drug-Naïve Schizophrenia Patients With Auditory Verbal Hallucinations. *Front Hum Neurosci* 2018;12:456; doi: 10.3389/fnhum.2018.00456.

**Table 1.** Descriptive table of demographic information

	<b>Tinnitus Group</b> <b>(N = 10)</b>	<b>Control Group</b> <b>(N = 10)</b>	<b>P value</b>
<b>Age (years)</b>	25.90 (5.49)	27.00 (4.71)	.63
<b>Sex (Male/Female)</b>	7/3	4/6	.06
<b>Hearing Thresholds (dB HL) (Right/Left)</b>			.451
250 Hz	10.00 (2.87)/11.25 (3.68)	13.50 (5.13)/10.00 (3.30)	
500 Hz	10.00 (2.07)/7.00 (1.97)	8.50 (1.85)/8.00 (1.78)	
1000 Hz	5.50 (2.05)/5.00 (1.90)	7.00 (1.83)/6.50 (1.68)	
2000 Hz	3.75 (1.94)/4.50 (2.47)	6.00 (1.72)/3.00 (2.20)	
3000 Hz	5.50 (2.46)/4.50 (2.81)	5.00 (2.20)/4.00 (2.53)	
4000 Hz	6.75 (3.30)/7.50 (2.58)	6.00 (2.93)/5.00 (2.31)	
6000 Hz	9.25 (3.38)/11.25 (3.47)	8.50 (3.04)/10.00 (3.10)	
8000 Hz	10.50 (2.97)/9.25 (3.89)	6.50 (2.65)/9.00 (3.48)	
<b>Mean Hearing Thresholds (dB HL)</b>	7.28 (4.72)	7.62 (4.72)	.882
<b>Tinnitus pitch (kHz)</b>	3.36 (2.84)		
<b>Tinnitus loudness (dB SL)</b>	24.33(14.85)		
<b>Tinnitus loudness VAS</b>	2.25 (1.22)		
<b>Tinnitus distress VAS</b>	1.13 (1.20)		
<b>THI</b>	29.00 (24.80)		
<b>TQ<sup>1</sup></b>	29.67 (12.88)		
<b>TFI</b>	27.48 (19.47)		

Notes: <sup>1</sup>TQ has one missing value. Data was present as Mean (SD).

## Figure Legends

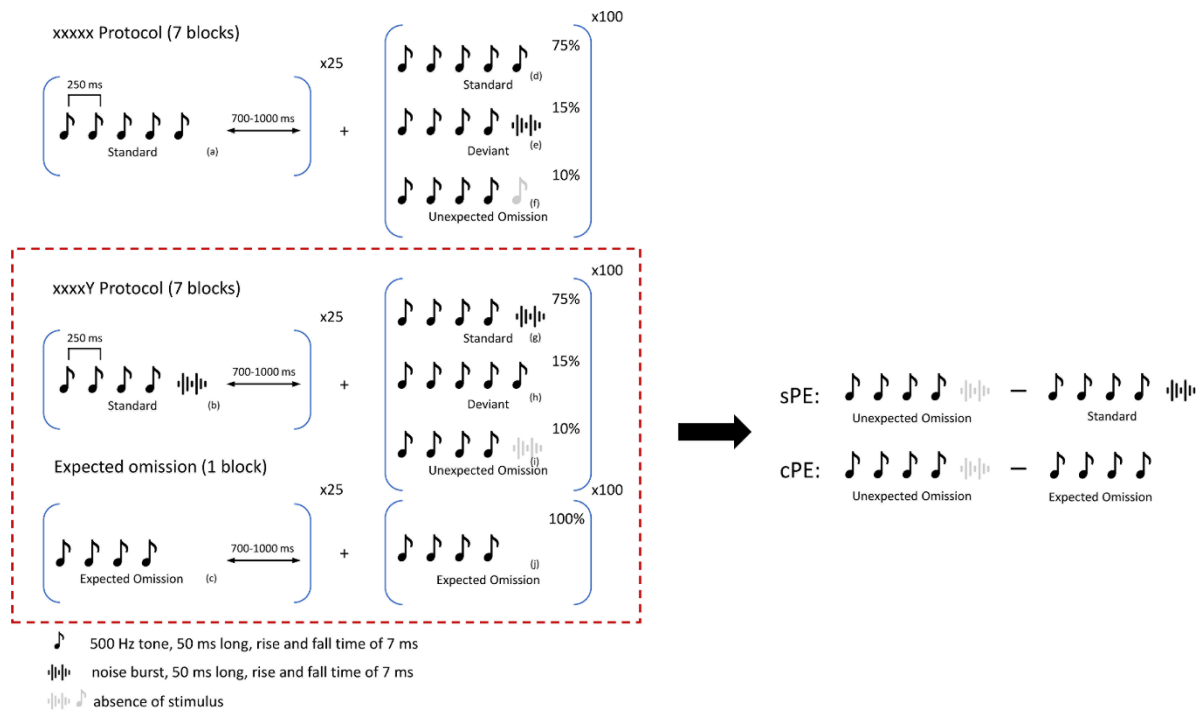


**Figure 1:** Auditory oddball paradigm. The full paradigm consists of three auditory stimulus sequences (a) a sound sequence with five monotonous stimuli, (b) a sound sequence with four tones and a noise burst, and (c) a sequence with four tones but absent fifth stimulus. The characteristics of stimuli are plotted at the bottom. In the xxxxx and xxxxy protocols, each block started with 25 trials of standard sequences. In the following 100 trials standard sequences (d,g) were presented with 75% probability, deviant sequences (e,h) with 15% and unexpected omission (f,i) as 10% probability. The omission protocol only consisted of omission sequences (j) with 100% probability. The red dotted box emphasised the protocol analysed in this study. Two prediction error (PE) conditions were generated by subtracting 1) stimulus-driven PE (sPE): unexpected omission and standard xY and 2) context-driven PE (cPE): unexpected omission and expected omission.

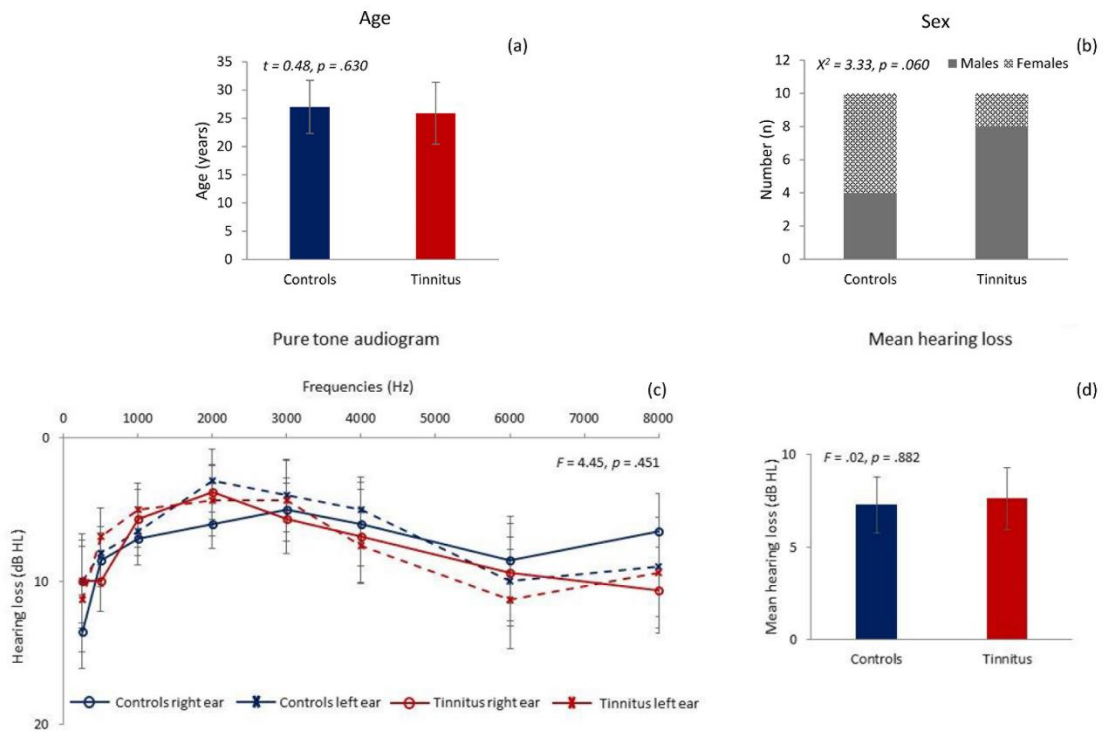


**Figure 2:** Comparison of the demographical characteristics between the tinnitus and control groups. (a) age, (b) sex, (c) pure tone audiograms and (d) mean hearing loss in db HL. Data were present as mean and error bars represent standard deviation.

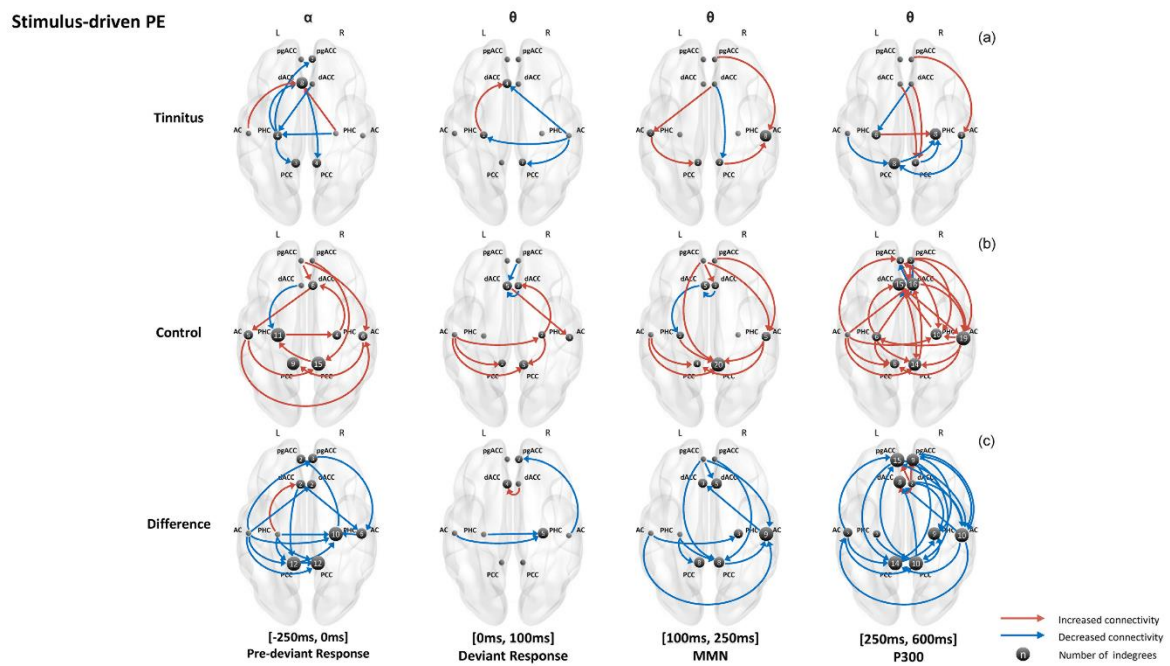


**Figure 3:** Summaries of connectivity network in the stimulus-driven PE. The figure displays the connectivity network for the tinnitus group (a), control group (b) and group difference (c) in the stimulus-driven PE condition. All connectivity are repetitive connections that occur two or more times within a specific timeframe. The connectivity network is in the alpha band during the pre-deviant response and in theta band in the following timeframes. The lines in red represent increased connectivity and blue ones are decreased. The sizes of nodes for each ROI are determined by the number of indegrees.

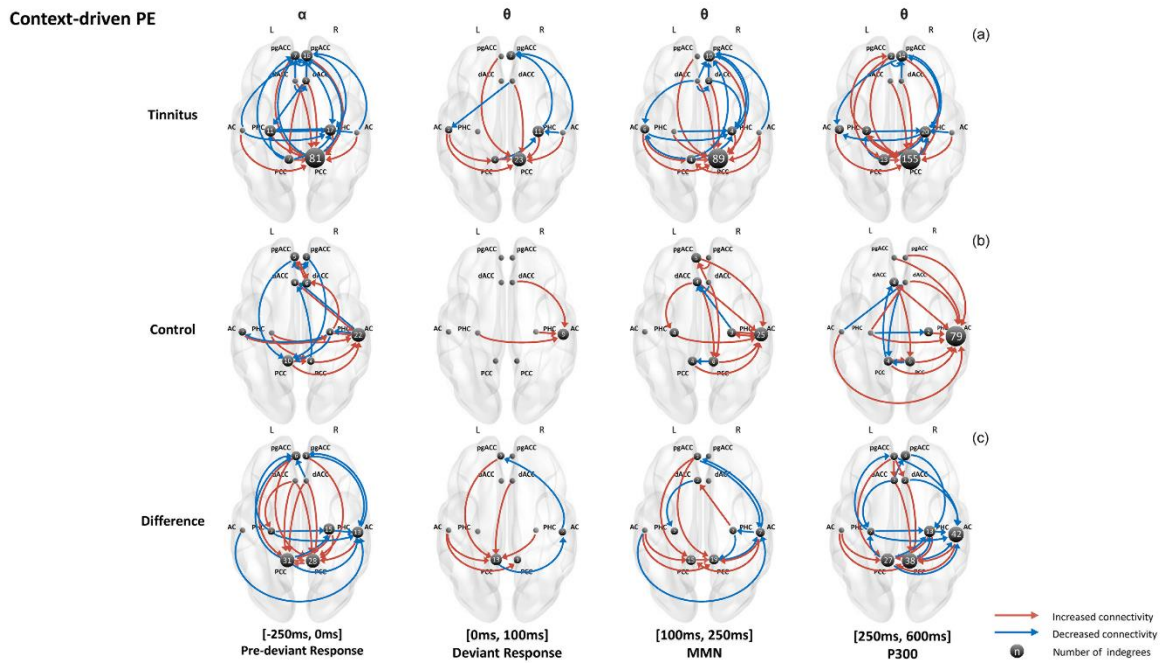


**Figure 4:** Summaries of connectivity network in the context-driven PE. The figure displays the connectivity network for the tinnitus group (a), control group (b) and group difference (c) in the context-driven PE condition. All connectivity are repetitive connections that occur two or more times within a specific timeframe. The connectivity network is in alpha band during the pre-deviant response and in theta band in the following timeframes. The lines in red represent increased connectivity and blue ones are decreased. The sizes of nodes for each ROI are determined by the number of indegrees.

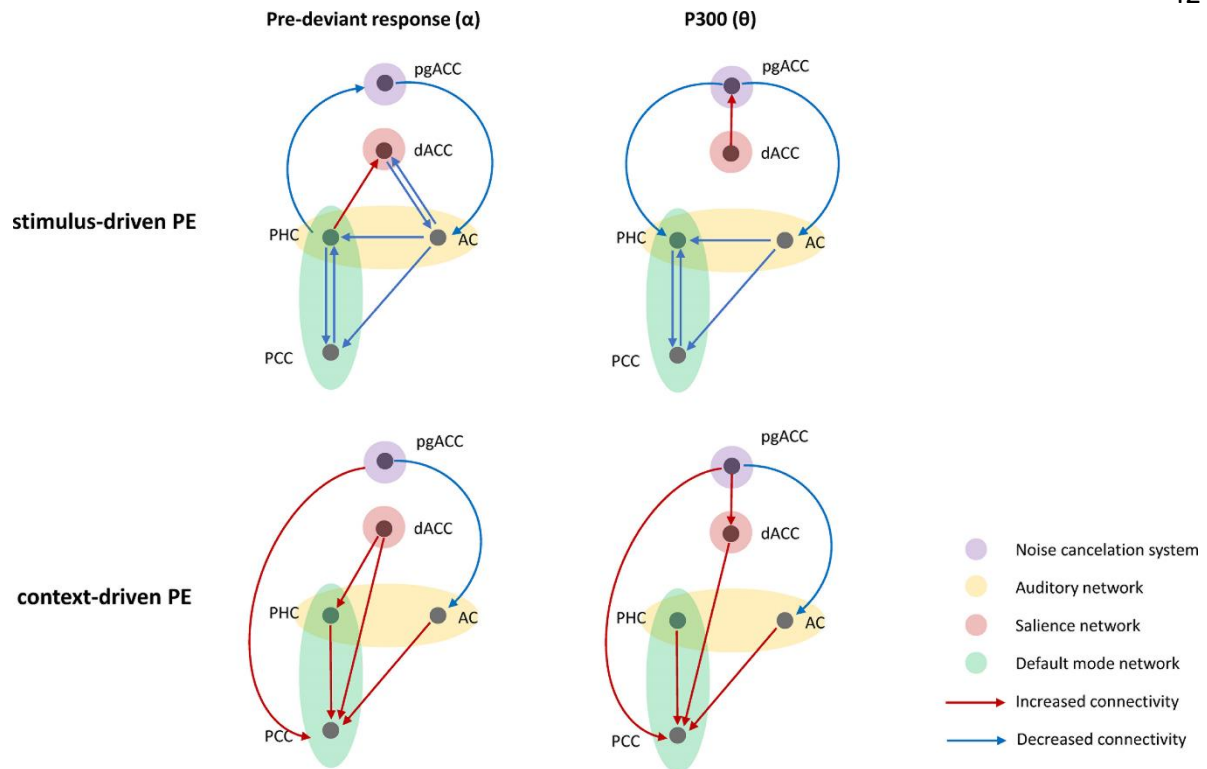


**Figure 5:** Graphical abstract showing the group difference between the tinnitus and control group for the pre-deviant and P300 time frames for the stimulus-driven and context-driven prediction errors. Red lines show increased connectivity for the tinnitus group than controls and blue lines show decreased connectivity. pgACC: pregenual anterior cingulate cortex; dACC: dorsal anterior cingulate cortex; PHC: parahippocampus; AC: auditory cortex; PCC: posterior cingulate cortex.